Magnetism and superconductivity in $C15$ compounds from self-consistent band calculations

T. Jarlborg
Physics Department, Northwestern University, Evanston, Illinois 60201

A. J. Freeman
Physics Department, Northwestern University, Evanston, Illinois 60201
and Argonne National Laboratory, Argonne, Illinois 60439

(Received 20 July 1979; revised manuscript received 27 February 1980)

All-atom–all-electron self-consistent semirelativistic linear muffin-tin orbital energy-band studies are reported for $TiBe_2$, $ZrZn_2$ (at ambient and high pressures), the high-T_c superconductor ZrV_2, and the ultralow-T_c superconductor YAl_2. Total and partial (by atom type and l values) density of states, Stoner-like parameters, electron-phonon coupling parameter λ and superconducting transition temperatures T_c (determined within the rigid muffin-tin approximation and McMillan's strong coupling theory with and without paramagnon contributions), and their behavior under applied pressure are used to discuss the origin of their observed magnetism and/or superconductivity. From an analysis of the results, we suggest possible high-T_c superconductivity at high pressure for $ZrZn_2$, and its unlikely occurrence for $TiBe_2$ unless dominant soft phonon modes exist.

I. INTRODUCTION

The cubic Laves or $C15$ compounds of type $MgCu_2$ exhibit a number of interesting phenomena including (i) the much studied weak ferromagnetism[1–9] in $ZrZn_2$ and (ii) correlations between high superconducting transition temperatures T_c and lattice instabilities[10–17] ZrV_2 and HfV_2, which are well known in the more familiar $A15$ and rocksalt transition-metal compounds. Interest in superconductivity and itinerant magnetism in the $C15$'s has recently been revitalized following the report of itinerant antiferromagnetism in $TiBe_2$ by Matthias *et al.*[18] This discovery followed the expectation raised by the theoretical proposal of Enz and Matthias[19] that the itinerant ferromagnetism of $ZrZn_2$ arises from inhibited "p-state" pairing. In this view, the Cooper pair interaction is thought to be repulsive at short distances (s state) due to a dominant soft phonon, leaving only p and high pair states to be attractive. Thus, the s-state repulsion would contribute to the Stoner factor sufficiently to tip the balance toward magnetism and to prevent the occurrence of p-state superconductivity. They further predict that above a critical pressure at which the magnetism is destroyed in $ZrZn_2$, p-state pairing superconductivity would appear and in $TiBe_2$ would coexist with any antiferromagnetic ordering.

Although extensively studied experimentally, only approximate model calculations[8,9] have been performed for the electronic band structure of $ZrZn_2$ treated as a diamond lattice of zirconium atoms with the zinc atoms entirely neglected. No energy-band studies have been made of $TiBe_2$ (or the high-T_c superconductors). Thus, it has not been possible to assess the possible electronic contributions to either a more conventional approach to superconductivity and/or magnetism or to the inhibited p-state pairing idea. This paper reports the first all-atom–all-electron, self-consistent semirelativistic energy-band calculations for $TiBe_2$, $ZrZn_2$ (at ambient and high pressures), the high-T_c superconductor ZrV_2, and the ultralow-T_c superconductor YAl_2. Total and partial (by atom type and l values) density of states (DOS), calculated Stoner-like parameters to study the conditions for magnetism, electron-phonon coupling parameters λ, and T_c values and their behavior under pressure are presented and used to provide a qualitative understanding of these phenomena including the possibility of superconductivity in $ZrZn_2$ and $TiBe_2$ with the application of pressure without invoking p-state pairing.

II. METHOD

The energy-band structures were determined self-consistently using the linear muffin-tin-orbital (LMTO) method.[20] The $C15$ (AB_2) structure is a very closely packed structure with 71% of the volume filled by touching spheres and the site symmetry is high for the two constituents. This makes the $C15$ structure especially suitable to study with the LMTO band method using spherically symmetric potentials. The basis set included s, p, and d orbitals ($l_{max}=2$) for each site, while the three-center terms included f

TABLE I. Calculated total and partial (by atom type and l value) density of states at E_F (per Ry cell) with a 3-mRy G broadening compared with the total DOS $N(\gamma)$ extracted from specific-heat data.

AB_2	As	Ap	Ad	Bs	Bp	Bd	Total	$N(\gamma)$
$TiBe_2$	0.2	20	91	1.5	23	4	140	480
$ZrZn_2$	0.2	23	79	1.2	20	3	126	440
ZrV_2	0.9	28	30	3.0	29	122	218	570
YAl_2	1.6	5	24	0.6	11	5	48	62

orbitals ($l'_{max}=3$) in the basis, in order to improve the basis-set convergence without increasing the dimension of the eigenvalue matrices.[21] The final self-consistent band calculations used an extended basis set with $l_{max}=3$, $l'_{max}=4$, in order to give reliable partial f-DOS functions. The self-consistent iterations used 16 k points in the irreducible Brillouin zone (IBZ) while the final band structure was determined at 85 independent k points. The overlapping Wigner-Seitz (WS) spheres used for these LMTO calculations were chosen by scaling touching muffin-tin (MT) spheres so that the total volume of all spheres equals that of the unit cell. Consequently the WS spheres are $0.242\,63a$ for A sites and $0.198\,14a$ for B sites, where a is the lattice constant.

The valence states were treated in a semirelativistic scheme,[22] where the mass-velocity and Darwin terms are included in the solution of the Dirac equation, but with the smaller spin-orbit terms excluded. The core states were treated fully relativistically and were recalculated in each iteration. The potential used in all cases was the Hedin-Lundqvist[23] local density formalism for the treatment of exchange and correlation. Other details of the band calculations are similar to those used earlier for $A15$ compounds[24] and ternary compounds.[25]

The final band results obtained at the 85 k points of the IBZ (same as for the fcc structure) were fitted to a Fourier-series representation to obtain band-structure plots, DOS diagrams, and Fermi-surface plots. It was found that 44 stars in the Fourier fit resulted in acceptable (1–2 mRy) rms errors, without causing any sever oscillatory behavior of the band fit. However, locally, at some symmetry points, the fitting errors reach about 10 mRy.

Results for total DOS data given here were determined from k-point weighted histograms using the Fourier fit and 4000 independent k points with a 1-mRy resolution and then broadened with a 3-mRy resolution function. The partial DOS diagrams, however, used the 85 k points directly without Fourier fitting using a 10-mRy energy mesh. The partial DOS values at the Fermi energy, given in Table I and used in the T_c calculations, were determined as an average of the values from moving the 10-mRy mesh in steps of 2 mRy, and then scaled so that the total DOS agrees with the total DOS obtained from the Fourier fit. (The scaling changed the DOS values typically by 5–10%.)

III. RESULTS

A. Band structure and magnetism

The energy-band structures of $TiBe_2$, $ZrZn_2$, and ZrV_2 are shown in Figs. 1–3 along the high-symmetry directions in the Brillouin zone. The plots are made from a Fourier series (44 symmetrized plane-wave) fit to the 85 independent *ab initio* k points. The conduction bands of $TiBe_2$ and $ZrZn_2$ are seen to be very similar (but note the high density of $3d$ bands of Zn at ~ 0.5 Ry below the Fermi energy, E_F). The ZrV_2 band structure (cf. Fig. 3) is seen to be quite different due to the large number of (flat) bands which exist at or below E_F—as is reflected also in the density of states.

We have determined the total and partial (by atom type and orbital angular momentum) density of states for $ZrZn_2$, $TiBe_2$, ZrV_2, and YAl_2 from k-point weighted histograms—as described above. As seen in Figs. 4 and 5, the Fermi energy E_F falls at or close to the top of a very narrow peak in the DOS. For $ZrZn_2$ the peak height is much lower than that of the model calculation by Koelling *et al.*,[8] which may be understandable because of their neglect of the Zn atoms. As shown in Table I and Fig. 4, this peak in both $ZrZn_2$ and $TiBe_2$ arises mostly from the Zr-Ti d bands; the Zn and Be p electrons, which are strongly hybridized with the Zr-Ti d electrons, make a non-negligible contribution at E_F. Such a high peak can easily lead to a strong temperature dependence observed for the resistivity and magnetic susceptibility and is an essential (but not sufficient) condition for

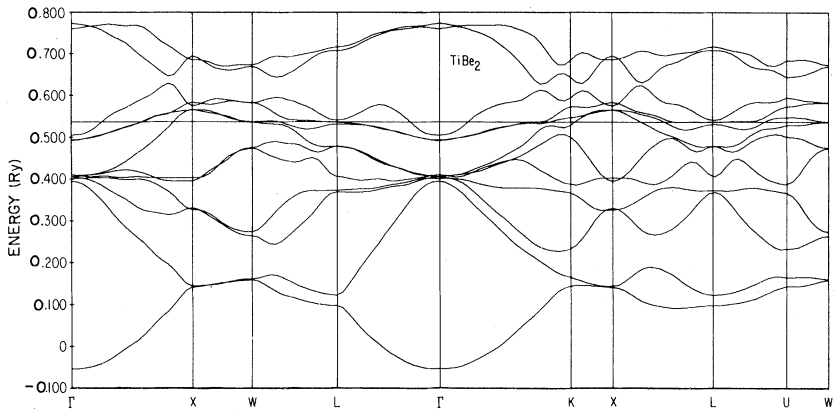

FIG. 1. The band structure for $TiBe_2$ obtained by a 44 star Fourier series to the 85 independent k points.

magnetism in Stoner theory.[4] Our calculated bare DOS at E_F, twice that of Pd, together with the measured susceptibility,[4,5] yields a large exchange enhancement[4] (~ 150 in $ZrZn_2$). This is consistent with an additional electron-electron and paramagnon enhancement of the electronic specific-heat coefficient, as found using our calculated λ value of 1.4 (cf. Table II). It is also consistent, except for ZrV_2, with the fact that our calculated λ values are well below the specific-heat-derived $\lambda(\gamma)$ values using our calculated $n(E_F)$ values.

In ZrV_2, E_F also falls on a narrow (but higher) peak in the DOS (cf. Fig. 6) which arises mainly from the V d electrons (cf. Table I). The Zr d-electron contribution is here much reduced from that in $ZrZn_2$ and is almost the same as that of the Zr p electrons (cf. Fig. 7 and Table I). In all three materials with a high DOS at E_F, it is the existence of a very flat band close to E_F centered mostly in regions near the L point (and along Γ-K in ZrV_2) which causes the sharp peak in the DOS and, in turn, some uncertainty in the exact position of E_F and the shape of the Fermi surface near the L point. By contrast, in YAl_2 E_F falls well above a (lower) DOS peak and is only 40% of the $ZrZn_2$-DOS value at E_F (cf. Fig. 6 and Table I). In general, our band results for YAl_2 agree reasonably well with Switendick's[26] non-self-consistent augmented plane-wave (APW) results.

The Fermi surfaces arising from the 4 bands which cross E_F in $TiBe_2$ and $ZrZn_2$, shown in Fig. 8, have strong similarities. The corresponding band structures (Figs. 1 and 2) show a very flat band (with a dispersion of only a few mRy in a large portion of the BZ) around the L point which just intersects the Fer-

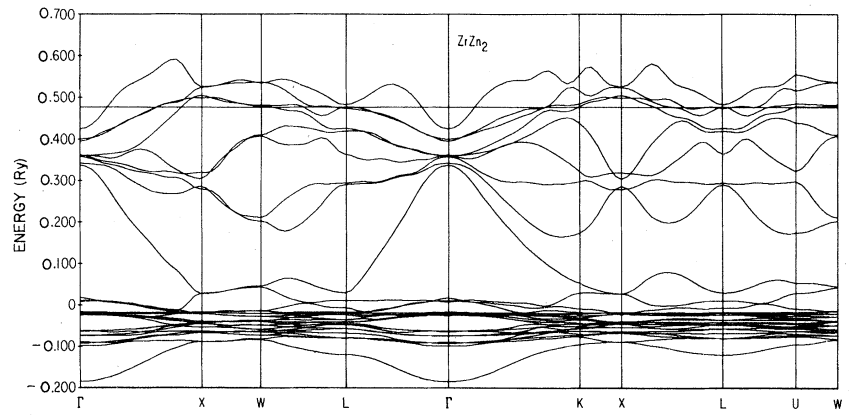

FIG. 2. The band structure for $ZrZn_2$ obtained by a 44 star Fourier series to the 85 independent k points.

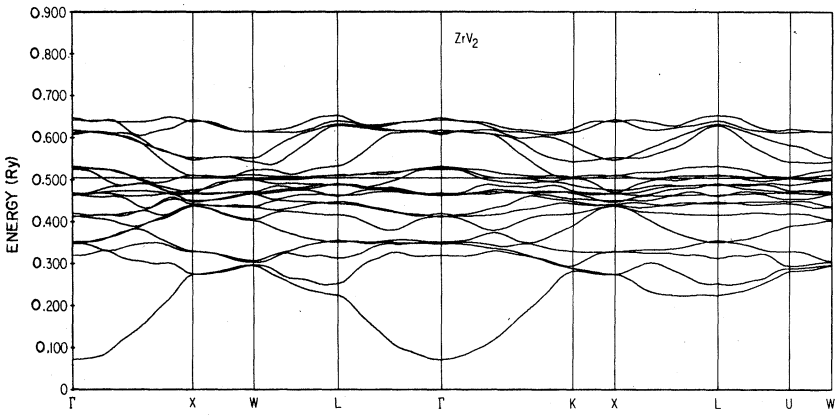

FIG. 3. The band structure for ZrV_2 obtained by a 44 star Fourier series to the 85 independent k points.

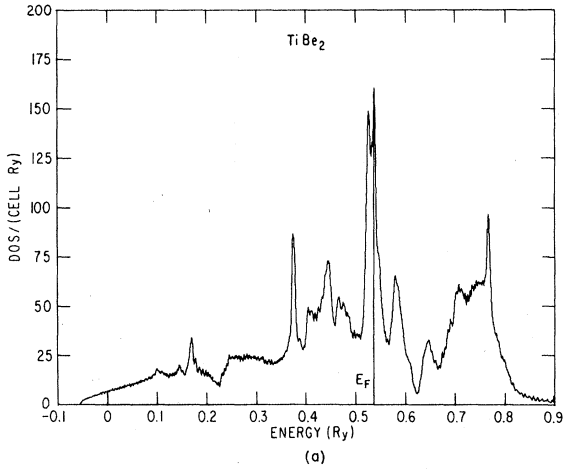

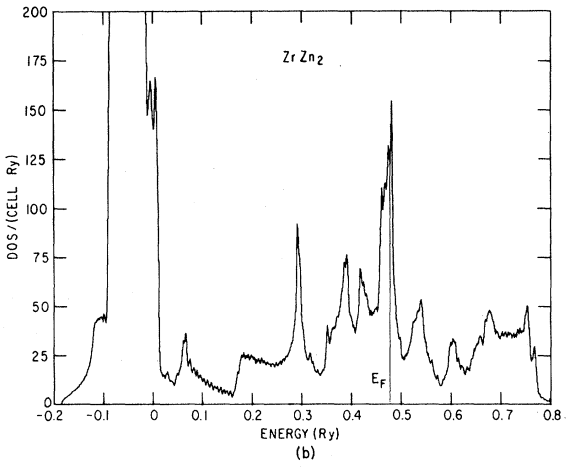

FIG. 4. Total density of states for $TiBe_2$ and $ZrZn_2$ determined from the Fourier-series fit and 4000 independent k points in the IBZ.

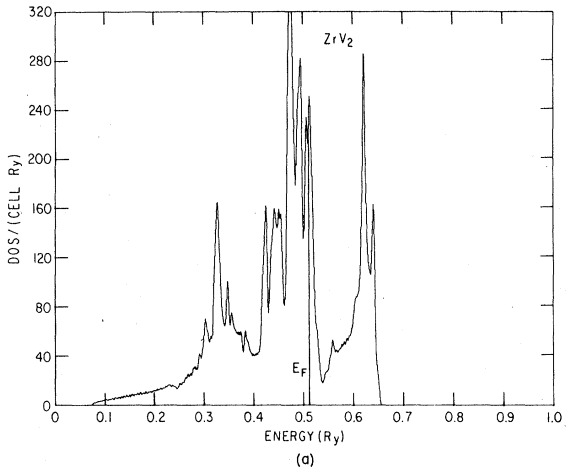

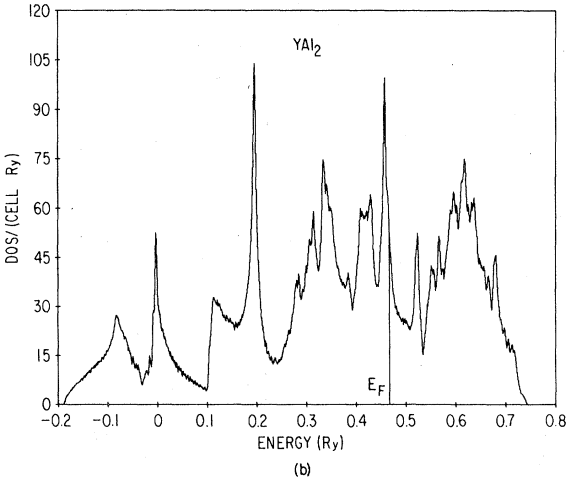

FIG. 5. Total density of states for ZrV_2 and YAl_2 determined from the Fourier-series fit and 4000 independent k points in the IBZ.

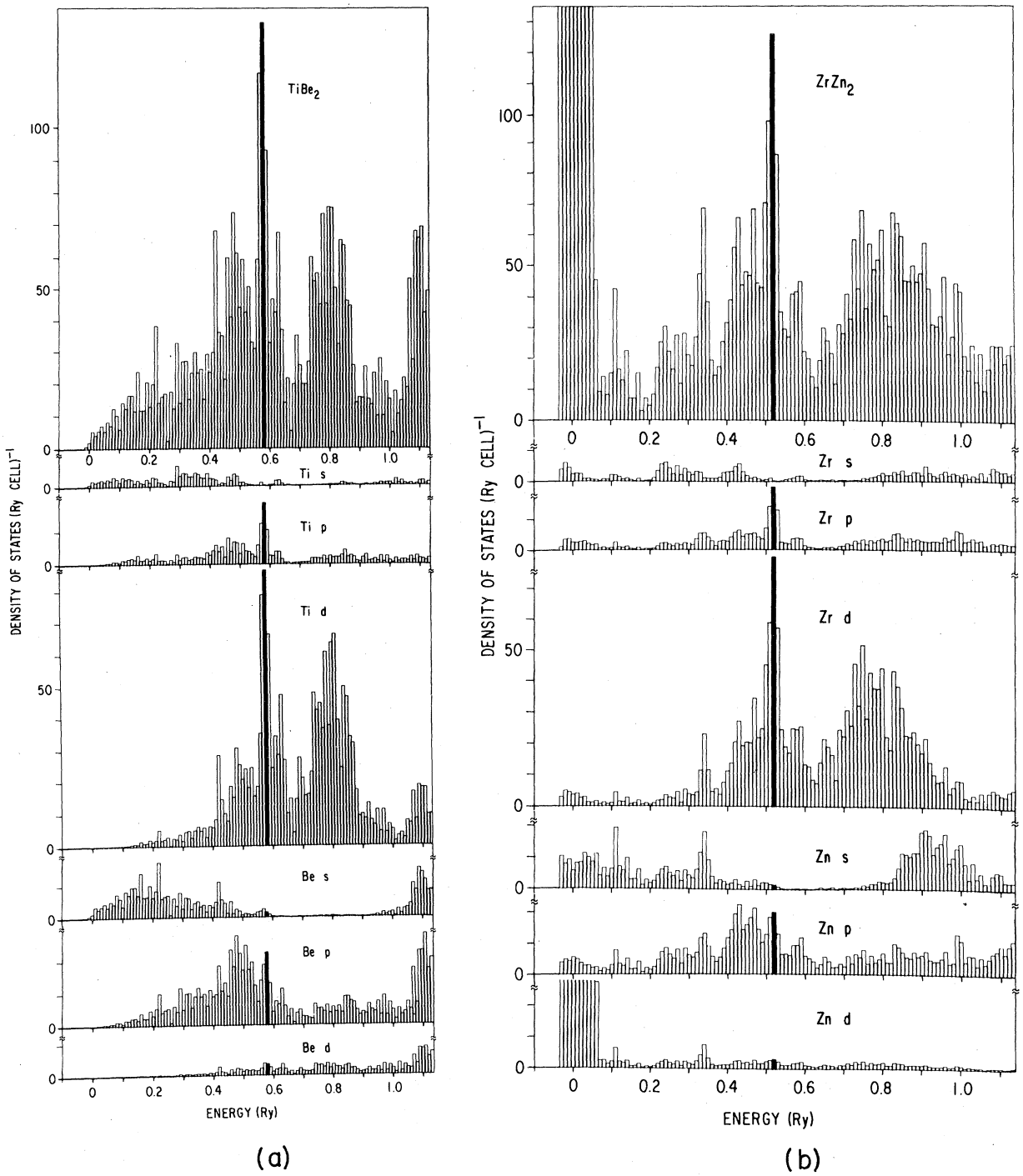

FIG. 6. (a),(b) Total and partial density of states for $TiBe_2$ and $ZrZn_2$ determined from 85 independent k points in the IBZ.

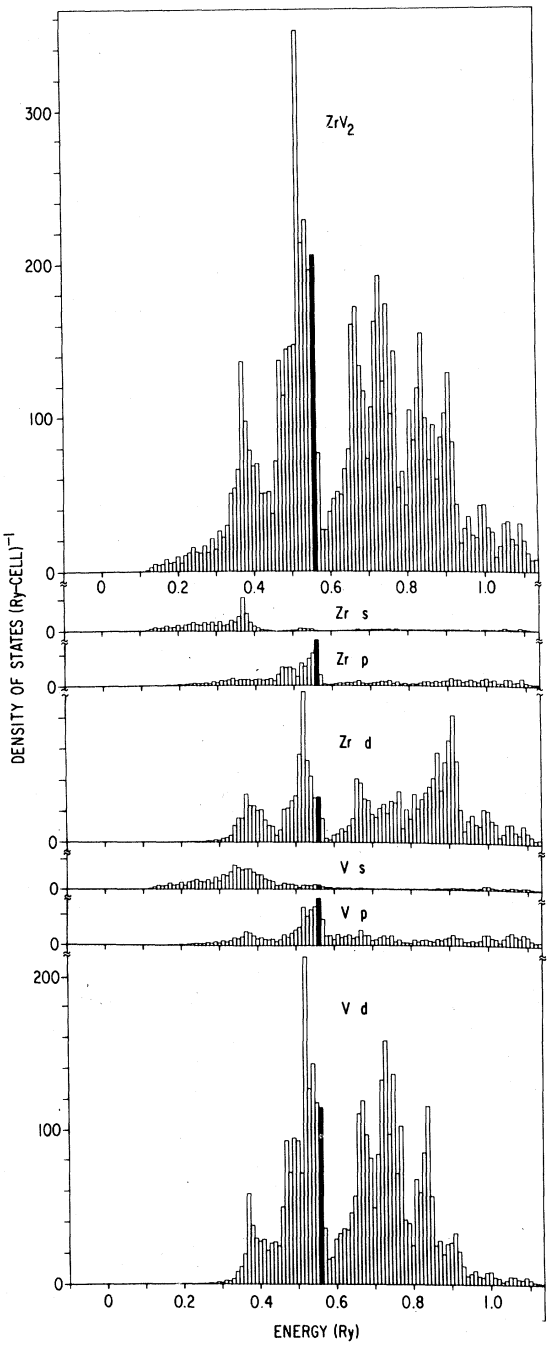

FIG. 7. Total and partial density of states of ZrV_2 determined from 85 independent k points in the IBZ.

mi level. As stated above, this band gives a large contribution to the DOS, but also introduces uncertainty about the exact shape of the Fermi surface around L. In addition, there are some differences in a band crossing E_F around the W-K region between $TiBe_2$ and $ZrZn_2$ which cause a somewhat different shape of the two Fermi surfaces in that region. Otherwise the Fermi surfaces for both compounds show considerable symmetry and strong nesting features of both intra- and interband types arising from 3 bands which form multiple "jungle-gyms" (of the type found in Pd and Pt), particularly along the Γ-X and Γ-K directions. Due to the differences around W, $TiBe_2$ has an ellipsoidal structure around the W-X-U line with greater overall nesting than in $ZrZn_2$. However, theoretical prediction of the occurrence of antiferromagnetic order in $TiBe_2$, as contrasted with the ferromagnetism observed in $ZrZn_2$, requires an accurate calculation of the wave-vector-dependent exchange-enhanced generalized susceptibility function, $\chi(\vec{q})$, given in random-phase approximation (RPA) as

$$\chi^0(\vec{q})/[1-\tilde{I}(\vec{q})\chi^0(\vec{q})] \ , \qquad (1)$$

where $\chi^0(\vec{q})$ is the noninteracting band susceptibility and $\tilde{I}(\vec{q})$ is the $\vec{q}$-dependent electron-electron interaction.

In analyzing our results for charge content (cf. Table II), we find a small charge transfer to Ti from Be and to Zr from Zn (0.07 and 0.16 electrons,

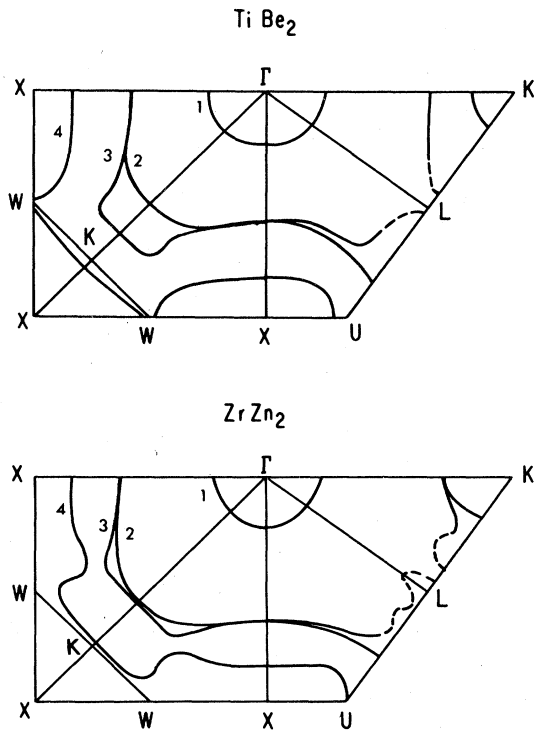

FIG. 8. The Fermi surface for $TiBe_2$ and $ZrZn_2$. The region around L has been drawn as dashed lines in order to indicate the uncertainty introduced by the presence of a flat energy band which just intersects E_F in this region.

TABLE II. Charge content (in electrons) projected by l value and atom type within each WS sphere, as obtained from the self-consistent results.

AB_2	As	Ap	Ad	Total	Bs	Bp	Bd	Total
$TiBe_2$	0.58	0.80	2.69	4.07	0.69	1.18	0.10	1.97
$ZrZn_2$	0.64	0.85	2.68	4.16	0.95	1.06	9.91	11.92
ZrV_2	0.76	0.92	2.79	4.46	0.60	0.55	3.61	4.77
YAl_2	0.60	0.81	1.99	3.39	1.06	1.50	0.25	2.81

respectively) and a moderate charge transfer from V to Zr (0.46 electrons). This transfer results in a total of 5.35 versus 5.59 Zr $4d$ electrons in $ZrZn_2$ and ZrV_2, respectively. The additional Zr $4d$ charge in ZrV_2 comes from hybridization and tail contributions from the vanadium $3d$ band. However, as shown in Fig. 9, the Zr $4d$ electrons at E_F are more localized in $ZrZn_2$ than in ZrV_2. The higher localization of the Zr $4d$ function in $ZrZn_2$ serves to increase the electron-electron interaction (relative to ZrV_2) and appears to contribute to an increase of the Stoner factor, making itinerant ferromagnetism considerably more likely in $ZrZn_2$ than in ZrV_2.

More specifically, the Stoner theory of magnetism offers a simple criterion for the onset of magnetic order. Writing the exchange-enhanced magnetic susceptibility as in Eq. (1) for the static ($q=0$) case

$$\chi=\chi_0[1-IN(E_F)]^{-1}=S\chi_0 \ , \tag{2}$$

where I is an effective electron-electron interaction, $N(E_F)$ is the DOS at E_F, and S is the exchange-enhancement (Stoner) factor, the magnetic instability occurs for $IN(E_F)\geq 1$. Janak[29] and others have determined I and $IN(E_F)$ for a number of elemental metals using local density theory. For compounds in which several atoms participate, each with sizable l-projected DOS, we need to derive a corresponding criterion for the onset of magnetic order. We start with the basic assumption that a small spin splitting ΔE is imposed on the band structure determined for the paramagnetic state. The occurrence of magnetism will be favorable if the resultant gain in exchange-correlation energy $\Delta\xi$ is greater than the loss of kinetic energy ΔT due to the spin splitting. If we assume that all bands are equally split, the kinetic energy difference is

$$\Delta T=\tfrac{1}{2}N(E_F)\Delta E\Delta E \ , \tag{3}$$

where $\frac{1}{2}N(E_F)\Delta E$ is equal to Δn, the number of electrons moved from one spin band to the other, and $N(E_F)$ is the total DOS at E_F. The $\Delta\xi$ is calculated in local density theory as the difference between the paramagnetic and ferromagnetic exchange-correlation energy due to the change in charge $\Delta\rho$ arising from Δn. Assuming a spherically symmetric spin density at a site t, the fractional magnetization can be written as

$$\zeta_t(r)=\frac{\rho_+-\rho_-}{\rho_++\rho_-}\approx\left[\sum_l N_{tl}(E_F)R_{tl}^2(E_F,r)\Big/\rho_t(r)\right]\Delta E \ . \tag{4}$$

Here N_{tl} is the local l-projected DOS at site t and $R_{tl}(E_F,r)$ is the radial wave function normalized to the Wigner-Seitz sphere at site t. The local spherical average of the spin density is written as

$$\Delta\rho(r)=\tfrac{1}{2}\sum_l N_l(E_F)R_{tl}^2(E_F,r)\frac{\Delta E}{4\pi} \ . \tag{5}$$

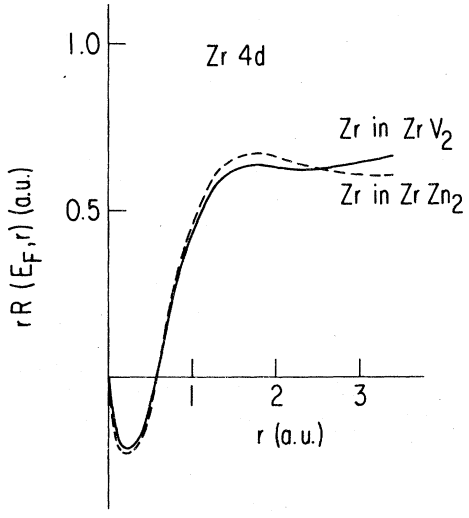

FIG. 9. The zirconium $4d$ radial wave function (times r) at the Fermi energy in $ZrZn_2$ (broken line) and ZrV_2 (full line). Note the relative localization of Zr in $ZrZn_2$.

Considering only the first order of the fractional magnetization[27] and using the local-spin-density functional of Gunnarsson and Lundqvist,[28] we can write

$$\Delta\xi_t = \frac{\Delta E^2}{8\pi}\int \Delta\rho(r)\mu(\rho)\tfrac{1}{3}\delta(\rho)\zeta(r)\,d^3r \ , \qquad (6)$$

where δ usually is expressed in the electron parameter r_s:

$$\delta(\rho) = 1 - 0.036r_s - 1.36r_s/(1+10r_s) \ . \qquad (7)$$

The density dependent parameter μ is the Kohn-Sham potential reduced by $\delta(\leq 1)$ due to correlation. Combining Eqs. (3)–(7) we calculate the criteria for magnetism as

$$\sum_t S_t = \sum_t \frac{1}{12\pi}\int_0^{R_{\rm ws}} r^2\mu(\rho)\delta(\rho)\left[\left(\sum_l N_l(E_F)R_{tl}^2(E_F,r)\right)^2\Big/\rho(r)\right]dr \geq \sum_t N_t(E_F) \qquad (8)$$

or

$$\sum_t S_t\Big/N(E_F) = \sum_t \bar{S}_t \geq 1 \ . \qquad (9)$$

Since the S_t integrals are quadratically dependent on the local DOS values, it is possible to write the condition (5) in the usual form

$$N(E_F)I \geq 1 \ , \qquad (10)$$

where I is essentially the S_t integral without the DOS factors,

$$I = \frac{1}{12\pi}\int_0^{R_{\rm ws}} r^2\mu(\rho)\delta(\rho)\frac{R_{tl}^4(E_F,r)}{\rho(r)}\,dr \ , \qquad (11)$$

when the t, l band is the dominating DOS at E_F. However, both conditions (9) and (10) scale linearly with the total DOS. The sum of $\bar{S}_t$ values are shown in Table III for $TiBe_2$, $ZrZn_2$ (at normal and reduced lattice constants), and ZrV_2. The calculations predict that $TiBe_2$ has a strong anomaly ($\bar{S}_{\rm tot}=1.22$) and $ZrZn_2$ ($\bar{S}_{\rm tot}=1.01$) a weaker one, while $ZrZn_2$ under pressure and ZrV_2 are nonmagnetic ($\bar{S}_{\rm tot}$ are 0.91 and 0.92, respectively).

To test the method, we have calculated effective I values for fcc Ni and Cu metals as $\bar{S}_{\rm tot}$ divided by the total DOS, obtained from separate self-consistent LMTO band calculations. We found the resulting I values to be about 5% larger than those of Janak. In Table III we also give the I values [from Eq. (11)] for the normalized $R_{tl}(E_F,r)$ functions to compare with the effective I values calculated by Janak[29] for the elemental metals. Our local I values are about 10% larger than those of Janak, but this is mainly due to differences in the d-wave functions and to Janak's use of the (adjusted, i.e., non-RPA) functional of von Barth and Hedin,[30] instead of the Gunnarsson-Lundqvist form.[27]

Comparing the local I_l values for Zr in $ZrZn_2$ and ZrV_2, it is evident that the exchange-correlation integral is reduced in the latter case by 5–10% due to

TABLE III. Normalized exchange-correlation energy integrals I_{tl} in rydbergs [from Eq. (11)], $\bar{S}_t$ values [from Eqs. (8) and (9)] times the number of atoms n_t in each unit cell and the total $\bar{S}$ values. The condition for magnetism is $\bar{S} \geq 1$.

		I_s	I_p	I_d	$\bar{S}_t n_t$	$\bar{S}_{\rm tot}$
$TiBe_2$	Ti	0.045	0.049	0.026	1.11	1.22
	Be	0.083	0.072	0.112	0.11	
$ZrZn_2$	Zr	0.034	0.038	0.023	0.96	1.01
	Zn	0.044	0.054	0.036	0.06	
$ZrZn_2(0.985)$	Zr	0.035	0.038	0.023	0.86	0.91
	Zn	0.043	0.051	0.035	0.05	
ZrV_2	Zr	0.032	0.035	0.022	0.20	0.92
	V	0.050	0.056	0.028	0.73	

the localization of the wave functions. Whereas the total DOS in ZrV_2 is very high, the DOS of Zr in ZrV_2 is lower than that of Zr in $ZrZn_2$ or of Ti in $TiBe_2$, and so the final $\bar{S}_t$ values are not high enough to give a magnetic instability. As expected from the higher local Ti-DOS in $TiBe_2$ than the local Zr-DOS in $ZrZn_2$ (cf. Table I), the magnetic anomaly is stronger in $TiBe_2$. In addition the lighter elements Ti and Be, with their lower charge densities, give larger normalized exchange-correlation integrals (by $\sim 50-80\%$) than are found for the heavier Zr and Zn atoms (see Table III).

Experimentally, it is found that the magnetism in $ZrZn_2$ disappears at an applied pressure of 8.5 kbars.[7] To our knowledge, a value of the bulk modulus for $ZrZn_2$ has not been measured; however, from the bulk-modulus data of Zr and Zn metals, a realistic number could be estimated to be around 1 Mbar. Thus, the 1.5% reduced lattice parameter would correspond to a pressure of about 50 kbars, which is much higher than the critical pressure of 8.5 kbars. From the calculated $\bar{S}_{\rm tot}$ values for $ZrZn_2$, at ambient pressure, and $ZrZn_2$ at 50 kbars in Table III, a $\bar{S}_{\rm tot}$ value of 1.00 is crudely interpolated to occur at ~ 5 kbars. However, with the numerical uncertainties involved in the DOS determinations, the approximations in the derivation of the Stoner-like criteria [Eq. (8)] with its sensitivity to the local spin-density functional, it is not realistic to place great credence on any calculated number of the critical pressure. Our model gives the observed order of magnitude because $ZrZn_2$ is close to the limit of magnetic ordering and hence it is likely that its magnetism will disappear at the moderately low pressure of the order of 10 kbars.

B. Electron-phonon coupling and superconductivity under pressure

Estimates of the electron-phonon coupling parameter λ and superconducting transition temperature T_c may be made using our band results, the crude rigid muffin-tin approxmiation,[31] and strong coupling theory.[32] The McMillan equation for strongly coupled superconductors expresses the superconducting transition temperature as[32,33]

$$T_c = \frac{\langle\omega^2\rangle^{1/2}}{1.20} \exp\left[-\frac{1.04(1+\lambda+\mu_{\rm sp})}{\lambda-(\mu^*+\mu_{\rm sp})(1+0.62\lambda)}\right] , \quad (12)$$

where $\langle\omega^2\rangle^{1/2}$ is the averaged phonon frequency and λ, μ, and $\mu_{\rm sp}$ are coupling constants for electron-phonon, electron-electron, and electron-spin interactions, respectively. The electron-phonon coupling parameter can be separated approximately into purely electronic (numerator) and purely phononic contributions (denominator):

$$\lambda = N(E_F)\langle I^2\rangle / M\langle\omega^2\rangle , \quad (13)$$

where M is the atomic mass. In our work, $\langle\omega^2\rangle$ is approximated by $\frac{1}{2}\Theta_D^2$ where Θ_D is the Debye temperature and the numerator is calculated by the rigid-ion formula of Gaspari and Gyorffy[31]:

$$N(E_F)\langle I^2\rangle = \frac{E_F}{N(E_F)\pi^2} \sum_l 2(l+1)\sin^2(\eta_{l+1}-\eta_l)\frac{N_l(E_F)N_{l+1}(E_F)}{N_l^0(E_F)N_l^0(E_F)} , \quad (14)$$

where η_l is the phase shift of the lth wave and $N_l^0(E_F)$ is the DOS for a single WS sphere. [Here Eq. (14) is used for quantities in WS spheres rather than in nonoverlapping MT spheres as in the original Gaspari-Gyorffy theory.] For μ^* we have used the empirical formula given by Bennemann and Garland[33] which relates μ^* to the calculated or "bare" total DOS $N(E_F)$ in units of (eV atom)$^{-1}$:

$$\mu^* = 0.26N(E_F)/[1+N(E_F)] . \quad (15)$$

In our calculations, μ^* values are in the range of 0.12–0.20 for low- (0.12) to high- (0.20) DOS materials, as compared with the original choice[32] of having $\mu^*=0.13$. Thus the use of Eq. (4) has essentially the same effect of suppressing T_c [cf. Eq. (12)] as does the use of $\mu^*=0.13$ and to introduce a spin paramagnon contribution $\mu_{\rm sp}\approx 0.07$ for the high-T_c materials. We consistently used Eq. (15) to determine μ^* while the effect from paramagnons $\mu_{\rm sp}$ was added as a separate contribution in a separate set of calculations labeled T_c^2 in Table IV. For the results listed, we used the partial DOS values obtained from the band results, averaged over 10 mRy, with the rigid-ion formula given by Gaspari and Gyorffy[31] to calculate the electron stiffness parameters $n\langle I^2\rangle$. In the final converged band calculations, the f states were included in the basis set, except for the $ZrZn_2$ calculations at reduced lattice parameters.

The results shown in Table IV must be viewed carefully because of various uncertainties in the calculations, including the sensitivity to changes in Θ_D. The trends and relative results given, however, are more meaningful. First of all, using a Θ_D for YAl_2 of[34] 470 K, we predict a very small T_c (<0.1 K) for YAl_2, which was found not to be superconducting above 50 mK.[34] In the case of ZrV_2, we used the geometric mean phonon frequencies of Hafstrom *et al.*[17] for HfV_2 scaled by the appropriate mass values, giving a Θ_D value to be 290 K, rather than

TABLE IV. Electron stiffness parameter $n\langle I^2\rangle$ (in units of eV/Å^2), electron-phonon-coupling constants λ_i separated by atom-type contributions, and estimated T_c values (in the absence of magnetism) using the Θ_D values shown. Values of T_c^1 are obtained *without* paramagnon contributions while T_c^2 used a μ_{sp} value of 0.10 for the high-susceptibility materials $TiBe_2$ and $ZrZn_2$ at normal lattice constant, and $\mu_{sp}=0.05$ in the other calculations. The total λ extracted from our total DOS and experimental specific-heat data γ is shown in the last column. Unlike Table I, these calculations used a 10-mRy average of the DOS functions. Note the different values of the lattice constants for $ZrZn_2$.

AB_2	n	$n\langle I^2\rangle_A$	$n\langle I^2\rangle_B$	λ_A	λ_B	T_c^1	T_c^2	Θ_D	$\lambda(\gamma)$
				0.51	0.03	~2	~0	650	
$TiBe_2$	130	8.8	0.09						2.7
				1.50	0.08	~25	~13	370	
$ZrZn_2(a)$	121	16.1	0.04	1.40	0.01	~24	~12	370	2.6
$ZrZn_2(0.9925a)$	117	15.1	0.04	1.22	0.01	~21	~15	390	
$ZrZn_2(0.985a)$	115	14.4	0.04	1.06	0.01	~17	~11	410	
ZrV_2	213	3.9	6.9	0.6	1.8	~32	~26	290	1.7
YAl_2	48	2.0	0.2	0.12	0.03	~0.1	~0	470	0.3

about 225 K obtained from specific-heat data.[11,13] For ZrV_2, we see that because of the high V-d DOS (cf. Table I) T_c is predicted to be very large (~32 K)—if the $C15$ phase is retained to low temperatures with unchanged lattice constant and geometric phonon frequencies.[12] The latter is an especially poor approximation, as can be seen from the Hafstrom *et al.*[17] data for HfV_2 which shows marked phonon hardening at the lowest temperature (~80 K) for which data have been obtained. Note that the electron per atom ratio in ZrV_2 is 4.67 and fulfills Matthias's valence rule for high-T_c materials.

This result for ZrV_2 is in sharp contrast to the results for $ZrZn_2$ and $TiBe_2$ where the dominant contribution to λ (and "T_c") is made by the high and narrow Zr and Ti DOS peak. Our calculations fulfill the Enz-Matthias[19] expectations in that a high "T_c" value (~24 K) is predicted if $ZrZn_2$ were an ordinary (i.e., nonferromagnetic) transition-metal compound. The suppression of the weak ferromagnetism with applied pressure is seen from Table IV as a direct consequence of the lowering of the DOS at E_F with pressure which rapidly (i.e., amplified by the exchange-enhancement factor) lowers the high Stoner factor. Our results at reduced lattice constants show that "T_c" still remains high (despite an assumed increase in $\frac{1}{2}\Theta_D^2$ by ~22%), indicating that $ZrZn_2$ might well become a high-T_c superconductor at high pressure—without invoking p-state pairing. As seen from Table IV, we find, using a recently measured Θ_D of 650 K,[35] that $TiBe_2$ at ambient pressure would have, in the limit of a complete absence of spin fluctuations, a small "T_c" ($T_c^1 \sim 2$ K).

To estimate the influence of spin fluctuations on calculated T_c values, we use Bennemann and Garland's[33] value of the electron-spin excitation coupling constant, $\mu_{sp}=0.05$ in all calculations of T_c^2 except $TiBe_2$ and $ZrZn_2$ at ambient pressure (where $\mu_{sp}=0.10$ is used). With the 0.05 values for μ_{sp} in the $C15$ calculations for T_c^2 [but still using Eq. (12) for determining μ^*] we obtain a reduction of 35–15% from the T_c^1 values. The calculated T_c^2 values obtained using a μ_{sp} value of 0.10, which is a realistic upper limit for high-T_c materials, give 50–30% reductions from T_c^1. These values give a lower limit to calculated-T_c values obtained in the rigid-ion approximation including paramagnon contributions.

To simulate the effect of soft phonon modes invoked by Enz and Matthias,[19] we also included in Table IV a calculation assuming the same Θ_D(370 K) (Ref. 36) for $TiBe_2$, as was used for $ZrZn_2$. Such a low Θ_D value gives very high values for λ and T_c. Hence, the search for soft modes takes on increased importance. Further, since moderate pressures would suppress possible magnetic effects (if any) on superconductivity without greatly suppressing our calculated "T_c" as in $ZrZn_2$, the search for superconductivity in $TiBe_2$ under pressure becomes an important undertaking.

ACKNOWLEDGMENTS

We are grateful to G. Knapp for close collaboration and discussions and to D. D. Koelling, B. Matthias, W. E. Pickett, and J. L. Smith for helpful discussions and unpublished reports. This research was supported in part by the Air Force Office of Scientific Research Grant No. 76-2948, the National Science Foundation Grants No. DMR 77-23776 and No. DMR 77-22646, through the Northwestern University Materials Reserach Center Grant No. DMR 76-80847, and the Department of Energy.

[1]B. T. Matthias and R. M. Bozorth, Phys. Rev. 109, 604 (1958).
[2]S. J. Pickart, H. A. Alperin, G. Shirane, and R. Nathans, Phys. Rev. Lett. 12, 444 (1964).
[3]S. Ogawa and N. Sakamoto, J. Phys. Soc. Jpn. 22, 1214 (1967); S. Foner, E. J. McNiff, Sr., and V. Sadagopan, Phys. Rev. Lett. 19, 1233 (1967); H. J. Blythe, J. Phys. C 1, 1604 (1968).
[4]E. P. Wohlfarth, J. Appl. Phys. 39, 1061 (1968).
[5]G. S. Knapp, F. Y. Fradin, and H. V. Culbert, J. Appl. Phys. 42, 1341 (1971).
[6]G. S. Knapp, E. Corenzwit, and C. W. Chu, Solid State Commun. 8, 639 (1970).
[7]T. F. Smith, J. A. Mydosh, and E. P. Wohlfarth, Phys. Rev. Lett. 27, 1732 (1971); J. G. Huber, M. B. Maple, D. Wohlleben, and G. S. Knapp, Solid State Commun. 16, 211 (1975).
[8]D. D. Koelling, D. L. Johnson, S. Kirkpatrick, and F. M. Mueller, Solid State Commun. 9, 2039 (1971).
[9]D. L. Johnson, Phys. Rev. B 9, 2273 (1974).
[10]A. C. Lawson, Phys. Lett. A 36, 8 (1971); A. C. Lawson and W. H. Zachariasen, *ibid.* 38, 1 (1972); A. C. Lawson, *ibid.* 38, 379 (1972).
[11]Ö. Rapp and L. J. Vieland, Phys. Lett. A 36, 369 (1971).
[12]D. E. Moncton, Solid State Commun. 13, 1779 (1973).
[13]T. Tokashima and H. Hayashi, J. Appl. Phys. Jpn. 12, 1659 (1973).
[14]T. Tokashima and H. Hayashi, Phys. Lett. A 47, 209 (1974).
[15]P. F. Schippnick and A. C. Lawson, Solid State Commun. 15, 1643 (1974).
[16]V. A. Finkel and E. A. Pushkarev, Sov. Phys. JETP 46, 1220 (1977).
[17]J. W. Hafstrom, G. S. Knapp, and A. T. Aldred, Phys. Rev. B 17, 2892 (1978).
[18]B. T. Matthias, A. L. Giorgi, V. O. Struebing, and J. L. Smith, Phys. Lett. A 69, 221 (1978).
[19]C. P. Enz and B. T. Matthias, Science 201, 828 (1978); Z. Phys. B 33, 129 (1979).
[20]O. K. Andersen, Phys. Rev. B 12, 3060 (1975).
[21]T. Jarlborg and G. Arbman, J. Phys. F 6, 189 (1976).
[22]D. D. Koelling and B. N. Harmon, J. Phys. C 10, 3107 (1975).
[23]L. Hedin, B. I. Lundqvist, and S. Lundqvist, Solid State Commun. 9, 537 (1971).
[24]T. Jarlborg, J. Phys. F 9, 283 (1979).
[25]T. Jarlborg, A. J. Freeman, and T. J. Watson-Yang, Phys. Rev. Lett. 39, 1032 (1977); T. Jarlborg and A. J. Freeman, *ibid.* 44, 178 (1980).
[26]A. C. Switendick, in *Proceedings of the 10th Rare Earth Conference* (Carefree, Arizona, 1973), p. 235.
[27]O. Gunnarsson and B. I. Lundqvist, Phys. Rev. B 13, 4274 (1976).
[28]O. Gunnarsson, J. Phys. F 6, 587 (1976).
[29]J. F. Janak, Phys. Rev. B 16, 255 (1977).
[30]U. von Barth and L. Hedin, J. Phys. C 5, 1629 (1972).
[31]G. D. Gaspari and B. L. Gyorffy, Phys. Rev. Lett. 28, 801 (1972).
[32]W. L. McMillan, Phys. Rev. 167, 331 (1968).
[33]K. H. Bennemann and J. W. Garland, in *Superconductivity in d- and f-Band Metals, Rochester, 1971,* edited by D. H. Douglas, AIP Conf. Proc. No. 4 (AIP, New York, 1972), p. 103.
[34]R. E. Hungsberg and K. A. Gschneidner, Jr., J. Phys. Chem. Solids 33, 409 (1972).
[35]G. R. Stewart, B. T. Matthias, A. L. Giorgi, E. G. Szklarz, and J. L. Smith, Solid State Commun. 30, 709 (1979).
[36]F. E. Hoare and J. C. G. Wheeler, Phys. Lett. 7, 402 (1966).